Ultrasonic and thermographic fatigue monitoring on a full-scale CFRP aeronautical component after repairing

Ultrasonic and thermographic fatigue monitoring on a full-scale CFRP aeronautical component after repairing

V Dattoma[1], R Nobile[1], F Palano[2], F W Panella[1], A Pirinu[1], A Saponaro[1,*]

[1]Department of Engineering for Innovation, University of Salento, Lecce 73100, Italy
[2]ENEA C.R. Brindisi - SS 7 km 706 - Brindisi - Italy

*e-mail: andrea.saponaro@unisalento.it

Abstract. The identification of defects in real components made in composite material assumes considerable importance in the aeronautical field, as irregularities in the material can compromise its functionality. Also, the possibility (NDT) to verify the effectiveness of repairing on the component during exercise through non-destructive testing techniques has great importance.
The goal of the present study is the application of the ultrasound and thermographic techniques for the identification of defects in a repaired component and the evaluation of the damage caused by the application of cyclical fatigue loads. All the important factors were studied, improving ultrasound scanning and allowing evaluating the effectiveness of the techniques used. In this paper, one case of study was proposed for non-destructive damage evaluation employing Phased Array ultrasonic and thermographic methods on aeronautical CFRP component. The structural element analysed is a spar with a double-T section with a hole and presents a repair by scarfing and hot bond process. The experimental results obtained shown the validity of the ultrasonic and thermographic technique for the sensitivity in detecting defects on full-scale aeronautical components with short execution and scan times.

Keywords: CFRP, aeronautical component, fatigue, ultrasonic phased array, thermography.

1. Introduction

Continuous carbon fiber composite with polymeric resin matrix (CFRP) provides lighter structural designs in both secondary and primary structural components, achieving lower fuel consumption and thus reduced emissions in aerospace applications [1]. The main mechanical characteristics of these materials could be briefly scheduled such as high strength-to-weight ratio, high stiffness-to-weight ratio, improved fatigue tolerance, corrosion resistance, formability and low thermal expansion [1]. Therefore, from a structural efficiency and safety viewpoint, the improvement of repair technologies for composite materials represents a recent research of industrial interest in order to ensure certified manufacturing quality (i.e. repeatable and defect-free processes) and verified mechanical properties of repaired structural parts [1, 2]. In fact, in a report of the US Government Accountability Office, the limited standardization of composite materials and repair techniques are identified as one of several important aviation safety-related issues [3]; therefore, the standardization of aeronautical repaired composite parts represents one of the major challenges for the aeronautical industry. During service life, damage mechanisms could occur in composite structure under static and dynamic loads and damage evolution process requires a suitable monitoring strategy by means of non-destructive techniques [2].

The optimization of damage detection techniques, in terms of resolution and costs, would enhance the performance of the structures. The most common investigation techniques are radiographic and ultrasonic techniques (immersion techniques, contact techniques and water jet techniques to transmit the ultrasonic signal from the probe to the material). Inspection techniques such as the phased array for ultrasonic investigations and thermography have a great potential in accelerating inspection processes [4, 5]. Several authors [4, 6, 7] make use of ND ultrasound systems using the modern phased array probe [6], for the reliable and effective detection of delaminations, which is the main damage modality for aeronautical components [8]. Therefore, recent research shows possibility of combining IRT technique with most accurate UT method for a complete characterization of real damage on CFRP parts after production issues, since IRT controls on relatively thin structural components were verified with consolidated ultrasound scanning [9], while ultrasonic systems are employed for the reliable and effective detection of in-depth composite delaminations [8, 10, 11] that are the main damage mode that occurs due to fatigue or impact phenomena [9].

In this work, ultrasonic with phased array technology and thermographic controls were performed on an aeronautical CFRP laminated component that has been subjected to a repair process. In particular, the structural component analysed is a spar with a double T-section that forms a part of the tail stabilizer of an aircraft. In order to validate the repair procedure, the beam has been tested according to a test protocol for the aeronautical sector, which has provided for fatigue tests, static tests and NDT to highlight any damage that occurred in correspondence of the repair. The ultrasonic controls to verify the quality of the repair with patches and the presence of any defects were carried out before performing the mechanical tests and after a certain number of cycles, in order to highlight defects induced by fatigue stresses. The results confirm the validity of the ultrasonic and thermographic inspection techniques for the sensitivity and the speed in detecting and characterizing defects in the repaired area of large-scale aeronautical components before the fatigue test and to in-situ fatigue monitoring: These techniques guarantee short execution and scan times and are in good agreement with the results provided by strain gages and rosettes, presented by the authors in previous works [12-16].

2. Materials and methods

2.1. CFRP aeronautical component

The test article is essentially a double T-section in CFRP, having upper and lower skins co-cured on the cap and a hole of about 100 mm in diameter on the core (Figure 1). Around hole, it has been simulated the presence of a damage, which has been repaired by scarfing and hot bond process to restore the structural integrity of the part. This technique is based on the application of a certain number of sub-laminates (called patches) that are polymerized and subsequently superimposed on the part to be repaired, interposing layers of adhesive [1].

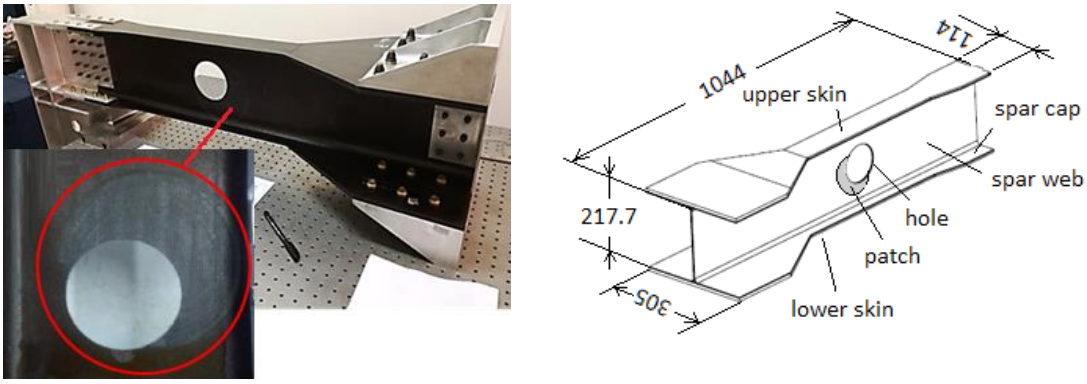

(a) (b)

Figure 1. Aeronautical spar: location of the repair (a) and geometry (b) (dimensions in mm).

The spar was subjected to random fatigue test. The ultrasonic control for checking the quality of the repair and detecting any defects was carried out before performing the mechanical test and during the fatigue test, in order to highlight any damage. The spar is principally constituted of two parts, the spar cap and the spar web. The cap part is realized with 10 plies, while the web part is built with 20 plies. Each ply has a nominal thickness of 0.186 mm. On spar cap a skin with a variable number from 50 to 28 additional plies were co-cured. This structural component is equipped at the two ends with aluminium supports fixed by rivets in Ti6Al4V that are used to constraint and load the spar during test. The information in terms of lamina properties constituents are shown in Table 1. Detailed information regarding materials and production processes are covered by a confidentiality agreement signed with the industrial partner of the research project.

Table 1. Number of plies and staking sequence for the constituent spar parts.

Part	Spar Cap	Spar Web	Skin Thin	Skin Big
Number of plies	10	20	28	50
Staking sequence	[45/-45/90/0/90/45/-45/45/-45/0]	([45/-45/90/0/90/45/-45/45/-45/0] s	([45/-45/0/45/-45/90/45/-45/0/-45/0/90/45/90] s	[45/-45/0/45/-45/0/90/45/-45/45/-45/45/0/45/90/0/-45/0/-45/0/-45/0/90/45/90] s

2.2. Pre-testing ultrasonic and thermographic controls

Preliminary ultrasonic and thermographic controls were carried out on repaired zone before fatigue and static test in order to evaluate the quality of the repair. UT phased array instruments (Olympus MX2 and MX) and an infrared camera (FLIR 7500M) were used to analyse the defects before performing the fatigue test and to monitor any damage caused by the subsequent fatigue cycles. Figures 2a and 2b show respectively the experimental set-ups with UT contact method and pulsed thermography before the mechanical tests. As shown in Figure 2b, the IR camera is positioned in front of the repaired patch as region of interest for the IRT controls and a suitable comparison with ultrasonic pre-test data. The spar width requires a camera-object distance of 410 mm for a correct thermographic evaluation.

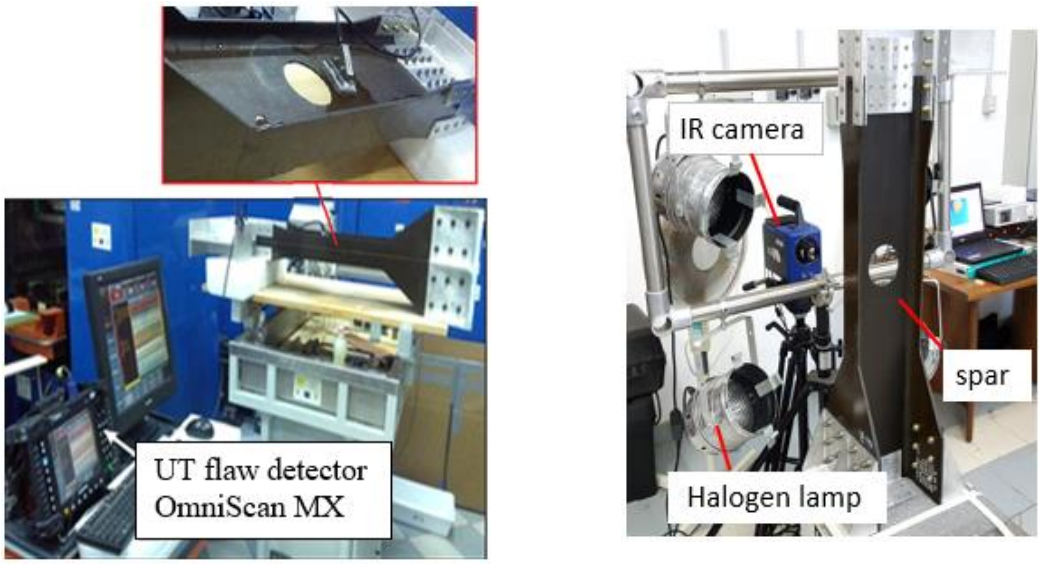

(a) (b)

Figure 2. (a) Experimental ultrasonic (a) and thermographic (b) set-up for the spar in pre-test control.

The phased array system consists in array transducers that physically use progressive waves, opportunely coordinated and shifted each other's. The wave-front generated by each element of the array at slightly different times combines with the impulses of the other elements to direct and shape the beam, in order to obtain a sharp focus and a different beam direction [4-6]. The Olympus OmniScan MX is used to perform the ultrasound analysis on the spar with the phased array technology, before fatigue test. It is equipped with an innovative probe of 64 elements that presents a frequency of 2.25 MHz. The probe is fixed on a plexiglass wedge.

The thermographic equipment consists of four halogen lamps, each with 1000 W power, controlled by a signal generator with single square wave of amplitude set to maximum lamp power and period calculated on the base of established heating time to synchronize thermal pulse and recording data. The adopted thermal camera is a FLIR 7500M IR camera , with a FPA cooled detector, endowed with NETD 25 mK In-Sb sensor and image resolution of 320 × 256 pixels; a processing data software ALTAIR provides thermal data in a 'ptw' video file and allows to convert the same to another format for custom processing [12]. All acquired thermal sequences are converted in 'ascii' files for a custom processing in Matlab environment. Previous experimental campaigns [12, 13] have defined optimal set-up for a better characterization of defects on similar CFRP plates, suitable thermographic parameters in terms of heating times in the range 12–40 s, capable to better identify defect depths in 2–6 mm range, experimental configuration distance, frame rate acquisition and lamps configuration.

2.3. Experimental set-up and fatigue test of composite patch/spar

Fatigue experimental activity has been scheduled by custom aeronautical company in order to evaluate a fatigue and static behaviour of the repaired component, validating its design and repair. Therefore, after preliminary Non-Destructive controls, the spar component has been equipped with 32 strain gauges and 10 rosettes with grids at 0° / 45° / 90°, as illustrated in Figure 3a. The strain gauges and rosettes were arranged in selected points of spar and a preliminary static test was conducted in order to verify the correct application of loads and constraints and to evaluate the resulting strain state, comparing the numerical results [14].

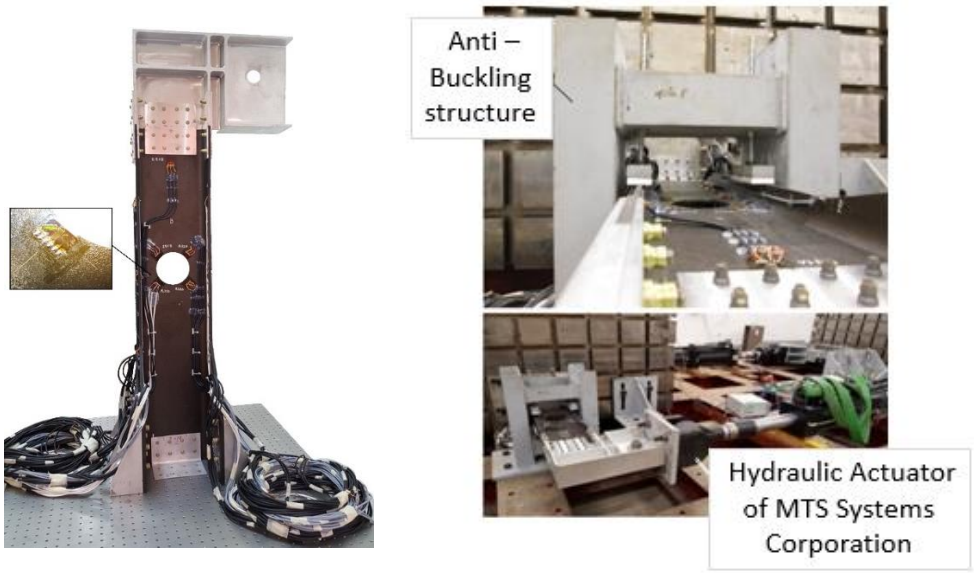

(a) (b)

Figure 3. (a) Front view of aeronautical spar with strain gauges and rosettes; (b) experimental set-up for spar's fatigue test with anti-buckling structure.

Mechanical tests and ND monitoring activities were carried out in the Structural Test Laboratory EMILIA of University of Salento (Casarano, Lecce (IT)). A spar extremity was fixed at a large cubic structure and transversally pin-loaded in bending at the other extremity by a hydraulic MTS actuator (maximum load capacity of 250 kN). As in Figure 3(b), a rigid metallic structure is used to avoid local buckling phenomena at the spar middle length.
Subsequently, the CFRP component was subjected to fatigue cycles that simulate the alternation between periods of flights, in which the spar works in the standard design conditions, and aerodynamic loads with totally absent wind or more turbulent winds [14]. Fatigue loads were scheduled by aeronautical company in order to evaluate the dynamic behaviour of a composite repaired spar representative of an aeronautical stabilizer. The fatigue cycles were carried out in load control using a test frequency of 0.5 Hz. Load history was obtained assembling six different load blocks of cycles for a total number of 90000 blocks and about 10^6 fatigue load cycles. During the load cycles, all strain gauges and rosettes data were recorded, measuring constant deformation amplitude for fatigue test duration. As a result, it was possible to verify the absence of expected changes in the structural behaviour of spar due to the applied load cycles.

2.4. UT and IRT monitoring of composite patch/spar during fatigue

In-situ ultrasonic and real-time thermographic monitoring was carried out on the patch to monitor any internal damage due to the application of the load cycles. Both acquisitions are recorded at predetermined intervals as 1000, 2000, 30000, 60000 block cycles and at the end of the fatigue test at 90000 block cycles with ultrasonic system OmniScan MX2 and FLIR 7500M thermal camera respectively. Figures 4a and 4b show the NDT configurations.

Whilst, the IRT monitoring controls requires a 45° angle for thermal camera on tripod due to steel anti-buckling support that interposed between thermal camera focus and region of interest (repaired patch, near the spar hole).

A manual ultrasound control was performed with phased array technique in reflection, optimizing the control parameters and using processing software for image analysis.

The ultrasonic control of the component was carried out manually by means of a system consisting of the OmniScan MX2 Olympus ultrasonic pulser and a 3.5 MHz and 64 elements phased array flat probe equipped with a suitable wedge, using a coupling gel between the probe and the sample surface.

The axial resolution of the PA probe used is about 0.3 mm, comparable with 1/3 of the ultrasonic wavelength in the investigated material, while the lateral resolution is 1 mm, since the probe's pitch is 1 mm.

The areas of interest investigated were those considered most critical both for the production process used and for subsequent mechanical tests. The analysed area is therefore the repaired zone and that adjacent to it.

Reference areas have been traced on the zone of interest in order to define numbered areas that can be easily identified from the position when the controls are carried during the mechanical test progress. The size of each rectangular area is equal to that of the probe endowed with wedge (approximately 35 x 66 mm^2).

Before performing the NDT on the component, it was necessary to perform a preventive calibration to establish the ultrasonic speed in the material (3030 m /s), the position of the back-wall echo and the wedge delay. The same gain value has been set for all ultrasonic inspections.
The ultrasound data were acquired, stored and processed by the MX2 instrument, which returns various graphic images of the examined part. The presence of strain gages and electrical strain rosettes on the test article, positioned to monitor the deformations during the execution of mechanical tests, it has significantly reduced the surface that can be investigated by ultrasonic inspection, respect to the inspection carried out prior to mechanical testing. In particular, the areas that could be inspected close to the repair were basically two: at the top and to the right of the hole on the web (Fig. 5). In detail, the surface at the top has been analysed with both horizontal and vertical scans. For the ND monitoring

performed at each interruption of the mechanical test, the same areas to be analysed were chosen, in order to define 11 areas that can be easily correlated with the position in which the check is carried out and compared with the progress of the fatigue test (Figure 5).

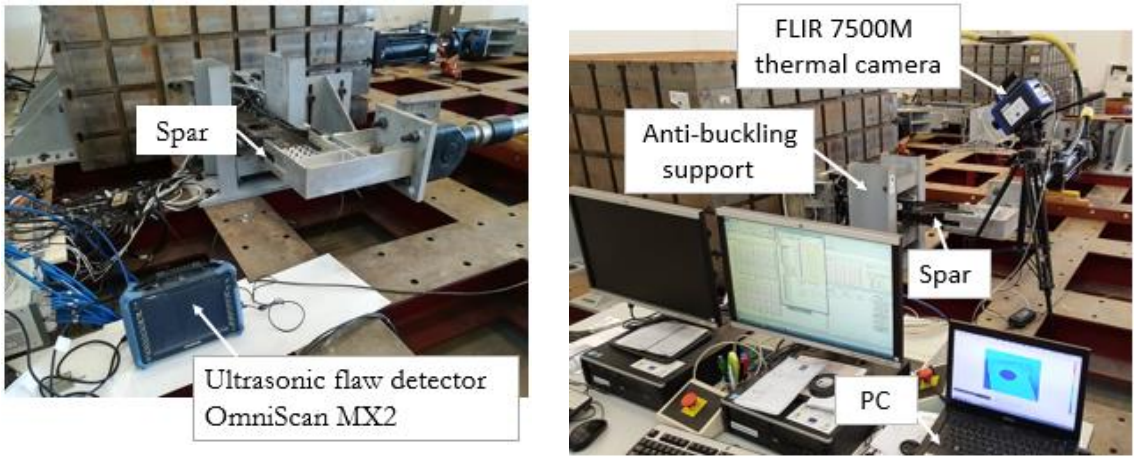

(a) (b)

Figure 4. (a) Experimental UT and (b) thermographic set-ups for the monitoring fatigue test of CFRP spar.

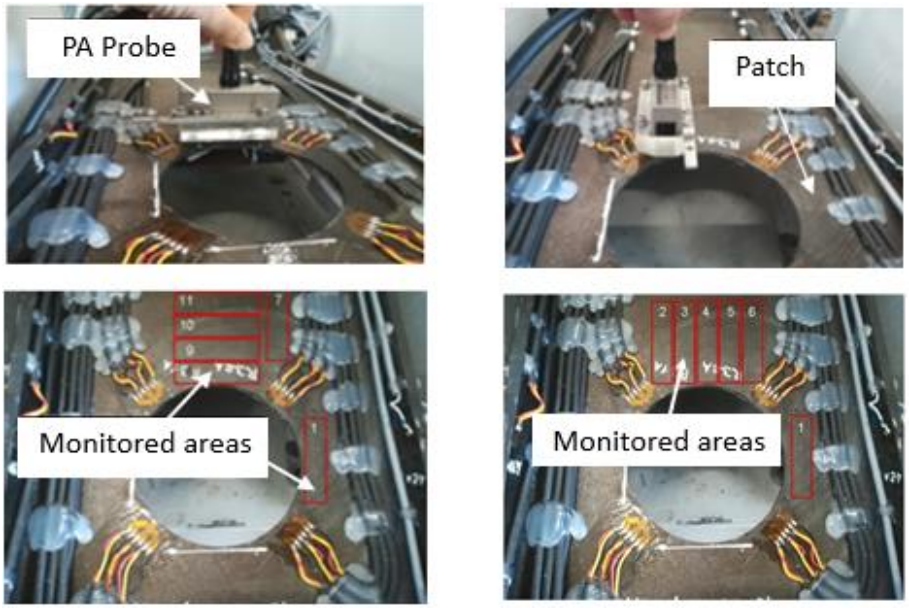

(a) (b)

Figure 5. Locations of monitored horizontal (a) and vertical (b) areas.

3. Results and discussion

The strain data have been acquired during bending fatigue cycles from strain gauges and rosettes positioned at the different zones. Strain analysis has assessed at the load values by the different strain gauges; strain data were almost constant during all sequence of fatigue cycles, suggesting the absence of damage [14]. ND investigation with UT and IRT techniques promise additional information on structural integrity of the spar before and during the fatigue tests.

The following sections describe detailed pre-test controls and monitoring results of both selected ND procedures, highlighting the effective correspondence of final data and the suitable strategy of combination controls.

3.1. UT and IRT pre-test analysis of the repaired spar

For the UT analysis of the spar, defects were firstly localized on the basis of cartesian coordinates and secondly characterized with the best probe in contact method. Cartesian coordinates are defined according to the inspection lines on the plane of the hole, one parallel to the spar longitudinal axis and the other normal. The inspection lines are equally spaced of 20 mm. The grayscale image was "rasterized" indicating the positions of the defects with a red square and the inspection lines with blue lines, as seen in Figure 6.

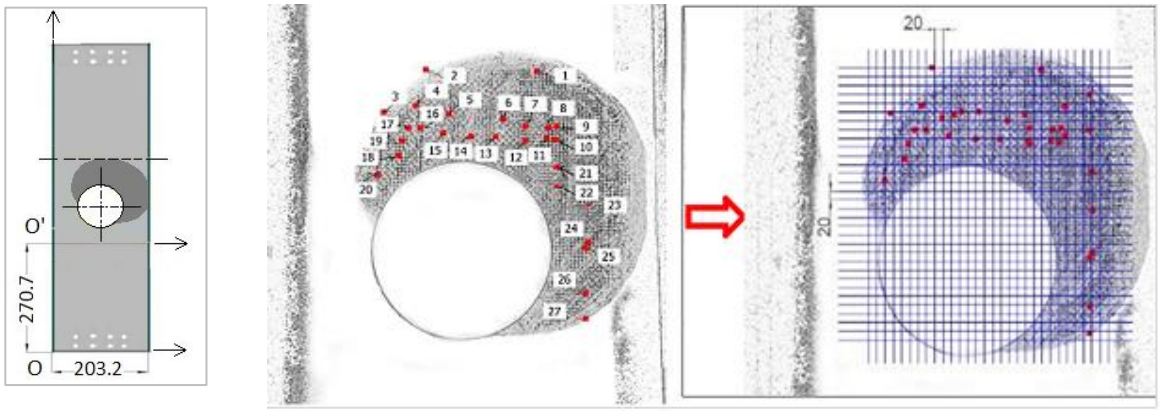

(a) (b)

Figure 6. Absolute and relative coordinate system (a); Defects detected with the grid of inspection lines near the patch around the hole (b).

The position of the potential defects detected in the relative reference system was subsequently associated with an absolute coordinate system taking into account the real dimensions of the component, as seen in Figure 6a. Twenty-seven defects have been identified at different depths between 0.7 and 2 mm, which can be characterized as micro-delaminations and voids in the patch. Figures 7 and 8 show some examples of defects found on the spar and marked in red.

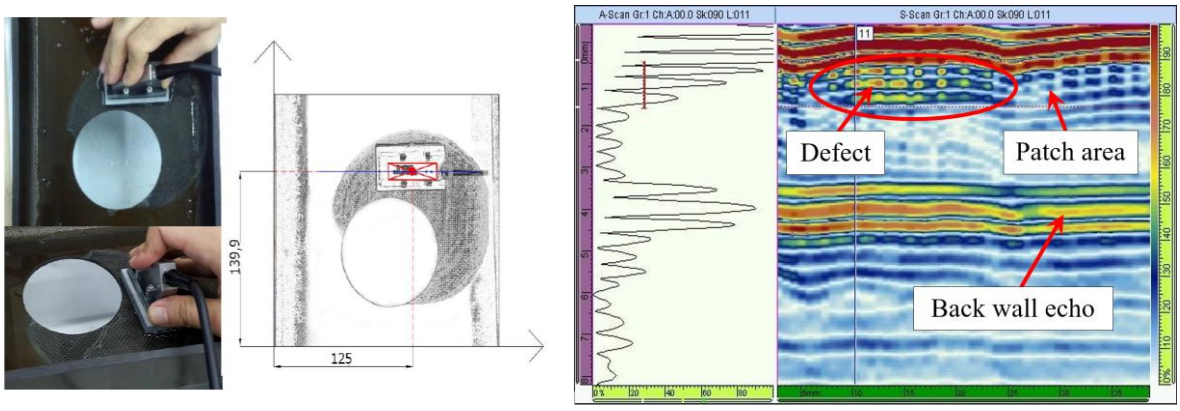

(a) (b)

Figure 7. (a) A-scan and S-scan (0°) for defect 6 and (b) A-scan and S-scan (0°) for defect 7.

The characterization of the detected defects was performed by recording the value of the amplitude, defined as the ratio between the defect's amplitude and that of the background echo, and the depth data, both obtained from the A-Scan. The advantage of the phased array probe lies in the immediate achievement of the sectorial scan that allows to better evaluating the shape of the defect compared to conventional probes. Table 2 summarizes some of the main significant defects found on the spar's repair.

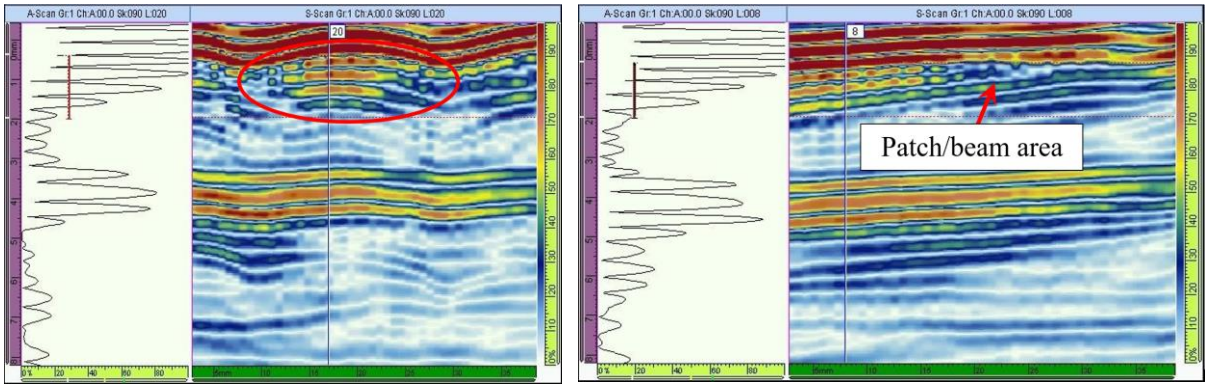

(a) (b)

Figure 8. A-scan and S-scan (0°) for defect 7 (a) and defect 11 (b).

Table 2. Summary table of the indications detected on the patch before the fatigue.

ID Defect	Relative coordinate [x, y]	Absolute coordinate [x, y]	Normalized amplitude [A/A (Bach-wall echo)]	Depth [mm]
1	(140, 164)	(140, 434.7)	38	0.9
2	(86.3, 164)	(86.3, 434.7)	45	0.85
3	(66.2, 164)	(66.2, 414.7)	68	1.1
4	(80.9, 148.6)	(80.9, 419.3)	82	0.8
5	(97.5, 144.4)	(97.5, 415.1)	54	0.8
6	(125, 139.9)	(125, 410.6)	78	0.95
7	(134.7, 136.2)	(134.7, 406.9)	90	0.8
8	(148, 136.2)	(148, 406.9)	56	0.9
9	(149.8, 136.2)	(149.8, 406.9)	68	1.3
10	(149.8, 131.8)	(149.8, 402,5)	64	1.8
11	(145, 131.8)	(154, 402.5)	99	0.8
12	(134.8, 131.8)	(134.8, 402.5)	95	0.7
13	(120.4, 131.8)	(120.4, 402.5)	82	0.9
14	(108.8, 131.8)	(108.8, 402.5)	66	1
15	(95.4, 131.8)	(95.4, 402.5)	47	1.55
16	(83.9, 135.8)	(83.9, 406.5)	76	1
17	(78.2, 135.8)	(78.2, 406.5)	56	1.3
18	(75.9, 129.8)	(75.9, 400.5)	72	1
19	(76.3, 130.2)	(76.3, 400.9)	66	1
20	(63.8, 113.5)	(63.8, 384.2)	40	2.5

The second pre-test control is conducted employing the Pulsed Thermography technique in reflection mode. Four tests are performed with 3, 5, 10, 15s heating times on the same region of interest of the scarfing repaired part, acquiring the thermal sequence with a frame rate of 5 Hz. The obtained heating of the surface's part was not uniform in all tests, due to the non-planarity of the scarfing repaired surface that presents a 'rectangular grid pattern' introduced by the repair technology, as shown in Figure 9a where the interwoven texture of the repair is thermally marked.

A qualitative thermal profile along the line 'd1' is selected in the thermogram of maximum heating time, as seen in Figure 9a; along the example thermal profile of Figure 9b, the temperature data show a curve variation around of 0.7 °C, detected symptomatic of the presence of defects.

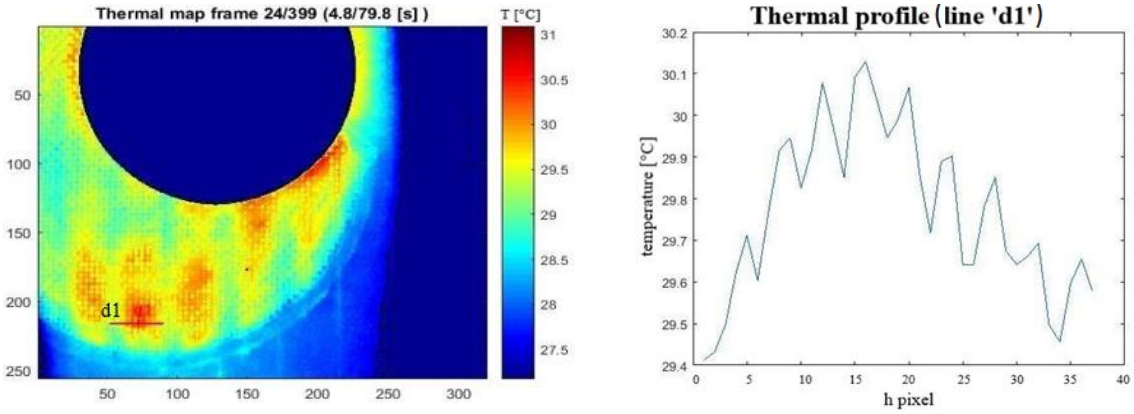

(a) (b)

Figure 9. (a) Thermal image employing a heating time of 5s; (b) thermal profile through the horizontal red line 'd1'.

Therefore, the normalized contrast C_n is selected for the thermographic analysis, in order to evaluate thermal data of selected zones minimizing thermal heating non-homogeneities along texture grid pattern. A Matlab algorithm was employed for C_n computation between the free- defect and the damaged zones, defined by the equation (1):

$$C_n(t) = \frac{\overline{T_d(t)}}{T_d(t_0)} - \frac{\overline{T_i(t)}}{T_i(t_0)} \quad (1)$$

where $\overline{T}$ represent the average temperature value of selected zones, t_0 is the maximum heating time, t is the time instant and d and i subscripts represent respectively the defective and free-defect areas. Figure 10a presents the selected Regions of Interest (ROIs) for normalized contrast evaluation of representative 3s heating time test because a low heating time provides both suitable information on possible presence of superficial defects and a useful comparison between IRT and UT results.

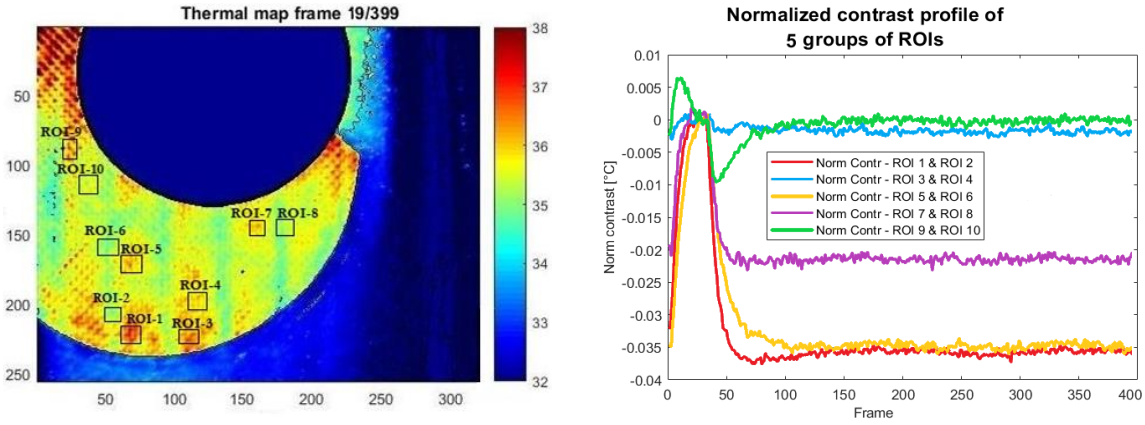

(a) (b)

Figure 10. (a) Thermogram with selected ROIs employing a heating time of 3s; (b) normalized contrast profile of selected ROIs.

Specifically, the odd numbers ROIs indicate the defective regions, while the near even numbers indicate the relative intact areas for the normalized contrast's calculation. Subsequently, the Matlab routine provides the normalized contrast diagrams of ROIs obtained during the thermal acquisition, as shown in Figure 10b for the chosen ROIs. Contrast profiles present similar trends tending initially towards zero at the maximum heating time (at 19th frame in this case) and then decreasing trend up to a constant equilibrium phase. The ROI-1 could be identified as the defect-1 by UT, although the other sub-superficial ROI-3, ROI-5 and ROI-7 defects seems not associable with previous detected defects.

3.2. Ultrasonic and thermographic monitoring results

Non-destructive tests (NDT) with ultrasound were carried out at intervals of 2000, 30000, 60000 and 90000 cycles. In order to monitor the test, the A-Scan and S-Scan (0 °) display modes were considered the most significant; in particular the S-Scans allow you to quickly compare the possible evolution of damage during the fatigue test. It can be seen from Figures 11 and 12 that the thickness of the patch is very irregular, as shown in the preliminary UT tests, but in correspondence with the Patch/beam bonding, of the area that has undergone the repair, there are no significant defects, not even as the fatigue test proceeds.

The gates have been positioned so that gate I is placed at the gel / material interface, gate B on the background echo and gate A inside the material, moving it according to the needs to display in the B-scan the particular investigated.

Higher signals (greater peak amplitude in A-scan) are revealed in B-scan with colours shifted towards yellow-red, while more attenuated signals (low signal amplitude in A-scan) with colours shifted towards green-blue.

The ultrasound representation reported in the results is the B-scan, as it is considered more significant to visualize any delaminations, voids or detachments of the patches.

OmniPC software allows offline processing of .opd data saved with the OmniScan MX2 system.

The application of the phased array reflection technique with a 64 elements 3.5 MHz flat probe represents a good monitoring technique to verify the adhesion of the repair to the component, as it has demonstrated the full control ability of a component in CFRP repaired with patch after scarfing.

It was possible to detect the presence of geometric irregularities of the patch surface and the absence of defects inside it and to verify the adhesion of the patch in service conditions.

In fact, this study shows that the irregular geometry of the patch material did not affect the strength of the component.

The irregularities reported could be the result of the production process of the beam or of the same material of which the patch is made. Figure 11 show as an example the ultrasound results relating to sector N ° 5 for each step of the fatigue test.

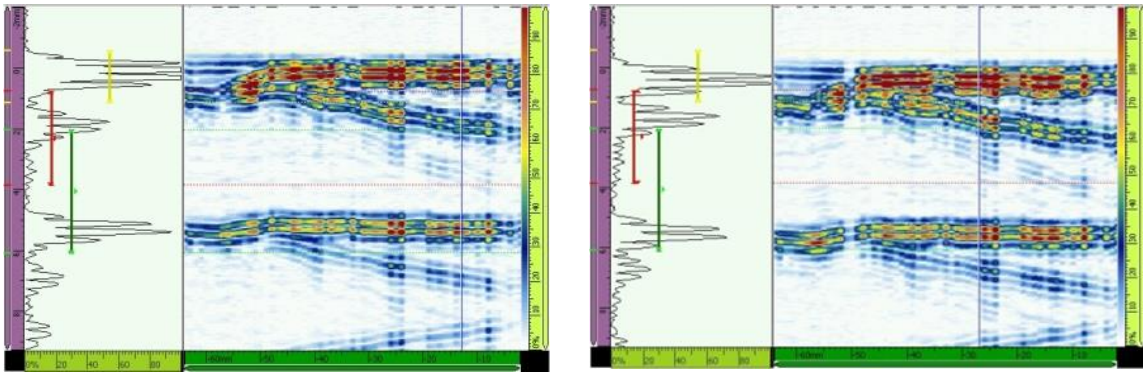

(a) (b)

Figure 11. Phased array results (A-scan and S-scan (0°)) at different fatigue cycles on the sector monitored N° 5. (a) 2000 cycles and (b) 60000 cycles.

Thermographic control consists on cycle-to-cycle monitoring near the hole zone with the repaired scarfing part, where the final failure should occur, acquiring the thermal data at each 1500 cycles with a frame rate of 100 Hz. Figure 12 shows two example thermograms relating to the initial and final cycle for the first load blocks; the surface heating obtained in all tests was not uniform, not only for the non-planarity of the blade surface, but also for the presence of strain gauges and related cables, which acts as thermal sources during measurement.

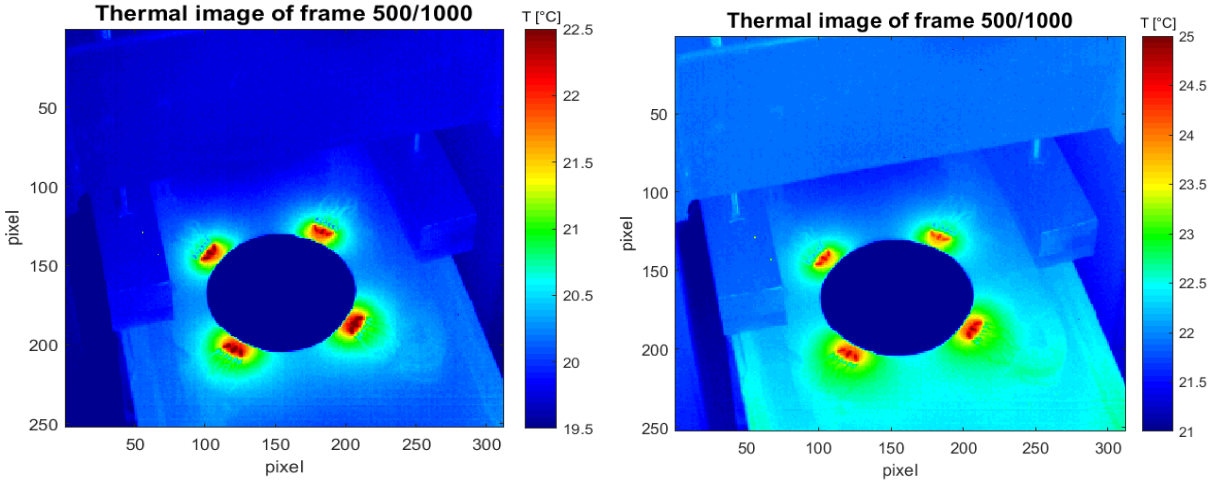

(a) (b)

Figure 12. Thermographic analysis of one loads' block at 3000 cycles (a) and 90000 cycles (b) on the monitored sector.

The thermal evaluation gives unsatisfactory information of internal spar structure and defective areas were not detected during fatigue test even after load cycles. As expected, the average temperature of the spar scarfing zone first undergoes a slow increase, then stabilizing around a constant value (Figure 12b).

4. Conclusions

The application of the infrared thermography and ultrasonic provide a suitable data comparison and useful ND strategy both for the preliminary controls and for experimental monitoring technique in the presented case of study. The superficial and in-depth structural integrity of the repaired component has been verified both in the preliminary pre-testing controls and during fatigue tests. Phased array ultrasonic technique allows the detection of small anomalies on scarfing patch's part of CFRP component; IRT controls presents a different distribution of sub-superficial defects except ROI-1, although the 'rectangular grid pattern' introduced by the repair technology. It was possible to monitor selected zones of the patch and to verify the adhesion integrity of the patch over time in service operating conditions. The combination of both ultrasonic and thermographic checks shows that the defects' presence within the patch material did not affect the strength of the component because the damage absence of structure is confirmed by both ND procedures during fatigue test.

Acknowledgements

This work has been financially supported by the project PON03PE_00067_2 Defect, damage and repair techniques in the manufacturing process of large composite structures (DITECO).

References

[1] Katnam K B, da Silva L F M, Young T M 2013 Bonded repair of composite aircraft structures: A review of scientific challenges and opportunities *Progress in Aerospace Sciences* **61** 26-42

[2] Baker A 1999 Bonded composite repair of fatigue-cracked primary aircraft structure *Composite Structures* **47 (1-4)** 431-443
[3] 2011 Aviation Safety: Status of FAA's actions to oversee the safety of composite airplanes *US Government Accountability of Office report: GAO-11-849* 1-50
[4] Bulavinov A, Kröning M, Pudovikov S, Oster R, Hanke R, Hegemann U, Reddy K M, Venkat R S 2008 Application of Sampling Phased Array Technique for ultrasonic inspection of CFRP components *International Symposium on NDT in Aerospace (Berlin)* 21-38
[5] Carofalo A P, Dattoma V, Palano F, Panella F W ND 2014 Testing Advances on CFRP with Ultrasonic and Thermal Techniques *Proceedings of ECCM 16 (Seville)* 1-8
[6] Ruiju H, Schmerr L W 2009 Characterization of the system functions of ultrasonic linear phased array inspection systems *Ultrasonics* **49** 219-225
[7] Kaczmarek H 1995 Ultrasonic detection of damage in CFRPs *J. Compos. Mater.* **29** 59-95
[8] Scarponi C, Briotti 2000 G Ultrasonic technique for the evaluation of delaminations on CFRP, GFRP, KFRP composite materials *Compos. Part B Eng.* **31** 237-243
[9] Bates D, Smith G, Lu D, Hewitt J 2000 Rapid thermal nondestructive testing of aircraft components *Compos. Part B Eng.* **31** 75-185
[10] Scarponi C, Briotti G 1997 Ultrasonic detection of delaminations on composite materials *J. Reinf. Plast. Compos.* **16** 768-790
[11] Jeong H 1997 Effect of void on the mechanical strength and ultrasonic attenuation of laminated composites *J. Compos. Mater.* **31** 277-292
[12] Dattoma V, Panella F W, Pirinu A, Saponaro A 2019 Advanced NDT Methods and Data Processing on Industrial CFRP Components *Applied Sciences* **9 (3)** 1-17
[13] Dattoma V, Panella F W, Pirinu A, Saponaro A 2020 Ultrasonic and thermographic studies for CFRP inspections with real and simulated defects *Materials today: proceedings* 1-11
[14] Castriota A, Dattoma V, Gambino B, Nobile R, Panella F, Pirinu A, Saponaro A 2018 Numerical and experimental analysis of a composite rear spar subjected to random fatigue loading conditions *Procedia Structural Integrity* **12** 71-81
[15] Casavola C, Palano F, De Cillis F, Tati A, Terzi R, Luprano V 2018 Analysis of CFRP joints by means of T-pull mechanical test and ultrasonic defects detection *Materials* **11 (4)** art. no. 620 1-17
[16] D'Accardi E, Palano F, Tamborrino R, Palumbo D , Tatì A, Terzi R, Galietti U 2019 Pulsed Phase Thermography Approach for the Characterization of Delaminations in CFRP and Comparison to Phased Array Ultrasonic Testing *J. of Nondestructive Evaluation* **38 (1)** art. no. 20 1-12